

Design of CDBA-based active polyphase filter for low-IF receiver applications

Mehmet SAĞBAŞ

Department of Electronics Engineering, Maltepe University,
34857 Maltepe, İstanbul-TURKEY
e-mail: sagbas@maltepe.edu.tr

Received: 28.12.2009

Abstract

A novel first-order active-RC polyphase filter section, using current differencing buffered amplifiers (CDBAs), is presented. The section uses 6 resistors, 2 capacitors, and 2 CDBAs. The transfer function of the proposed section has a single pole and optionally a single zero. Increasing the number of cascading sections, any higher order polyphase filter can be realized. This paper also introduces the leakage caused by element deviation and the effects of the amplifier in nonideal cases. Furthermore, nonideal performances of the proposed filter section are tested with PSpice simulations.

Key Words: Active polyphase filters, current differencing buffered amplifiers, active filters, complex filters, low-IF receivers

1. Introduction

Polyphase filters are indispensable for recent wireless communication systems. They are used for in-phase and quadrature-phase signal generation and image rejection in the analog front end of radio frequency integrated wireless transceivers [1-3]. RC-polyphase filters were employed in the 1970s [4,5]. Today's applications of polyphase filters are based on zero- and low-IF receivers. The asymmetric polyphase filter makes it possible to suppress the mirror signal not only at high frequency, but also after quadrature demodulation at a low intermediate frequency (low-IF). Integrated circuit implementations of the polyphase filters are state of the art [6-8].

Polyphase filters can be either passive or active. Passive polyphase filters are built of only resistors and capacitors [1,7,8]. Active polyphase filters consist of gain blocks with resistors and capacitors. One of the main advantages of active over passive polyphase filters is that active polyphase filters are more suitable for monolithic integration than their passive counterparts [6]. Another advantage of active over passive polyphase filters is that, in a receiver, a small wanted signal can be surrounded by large neighboring signals, and this requires a very high dynamic range at the input. Such high levels of dynamic ranges can only be achieved using active-RC techniques [9]. Although passive polyphase filters employing only resistors and capacitors have been

widely used [1], their design for higher orders is considered complicated due to the absence of the cascading concept to avoid loading effects [2].

Therefore, active polyphase filters have emerged using op-amps [9-11], operational transconductance amplifiers [12-15], current mirrors [16], second generation current conveyors [17], and current feedback operational amplifiers [18,19]. However, the performance of current conveyor-based circuits has an advantage over that of conventional operational amplifier circuits, which have limited bandwidth at high closed-loop gains due to the constant gain-bandwidth product. Furthermore, the limited slew rate of the operational amplifier affects the large-signal, high-frequency operation. When wide bandwidth, low power consumption, and low voltage operation are needed simultaneously, the voltage-mode operational amplifier becomes very complex [20]. These disadvantages can be eliminated using current conveyors or current conveyor-based active elements [21-23]. The performance of current conveyor-based circuits, in terms of bandwidth, linearity, and dynamic range, is also better than that of OTA-based circuits [24].

In this paper, a design methodology for an active-RC polyphase filter section using CDBAs is presented. While several quadrature oscillators using CDBA have already been reported in the literature, this paper extends similar applications to polyphase filters [28,29]. The proposed circuit employs 6 resistors, 2 grounded capacitors that are suitable for IC implementation, and 2 CDBAs.

2. Realization of active polyphase filter

A CDBA is a 5-terminal (2 inputs, 2 outputs, and 1 ground) active element that can be used in current-mode and voltage-mode analog signal processing circuits and filters [25,30-32]. The p -terminal of the CDBA is positive (noninverting) input and the n -terminal is negative (inverting) input. Both of the input terminals are internally grounded, which makes them preferable current inputs. The z -terminal is a current output and the w -terminal is a voltage output that follows the potential at the z -terminal with respect to the ground, which is why it is called voltage output. Low impedance inputs at the p - and n -terminals with high impedance output at the z -terminal make the CDBA a suitable cascading active element in the current mode. Furthermore, a low impedance output at the w -terminal is suitable for a cascade connection when operating in the voltage mode. The block diagram of a CDBA is shown in Figure 1. Its ideal current and voltage characteristics can be described by:

$$V_p = 0, V_n = 0, I_z = I_p - I_n, V_w = V_z. \quad (1)$$

Taking the nonidealities of the CDBA into account, the above terminal equations can be rewritten as:

$$V_p = 0, V_n = 0, I_z = \alpha_p I_p - \alpha_n I_n, V_w = \beta V_z, \quad (2)$$

where α_p and α_n are the current gains and β is the voltage gain. These gains can be expressed by using the current tracking errors $|\varepsilon_p| \ll 1$ and $|\varepsilon_n| \ll 1$ and the voltage tracking error $|\varepsilon_v| \ll 1$ as $\alpha_p = 1 - \varepsilon_p$, $\alpha_n = 1 - \varepsilon_n$, and $\beta = 1 - \varepsilon_v$.

According to the above equations, this element converts the difference of the input currents I_p and I_n into the output voltage V_w through the impedance, which will be connected to the z -terminal. Therefore, the CDBA can be considered as a transimpedance amplifier, and from this viewpoint, it is similar to a CFA [26]. Besides, the differential nature at the input makes this element especially suitable for fully integrated filter implementations [32].

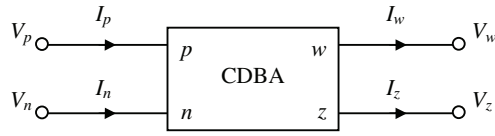


Figure 1. Block diagram of CDBA.

Figure 2 shows the structure of a low-IF receiver using a polyphase filter, which is used in both I and Q channels [7,8]. According to Figure 2, the low-IF receivers comprise a low noise amplifier (LNA), which amplifies the RF signal and sends it to a RF quadrature mixer, which downconverts the RF signals to IF. A polyphase filter, which follows the mixer, rejects the image and performs the channel selection.

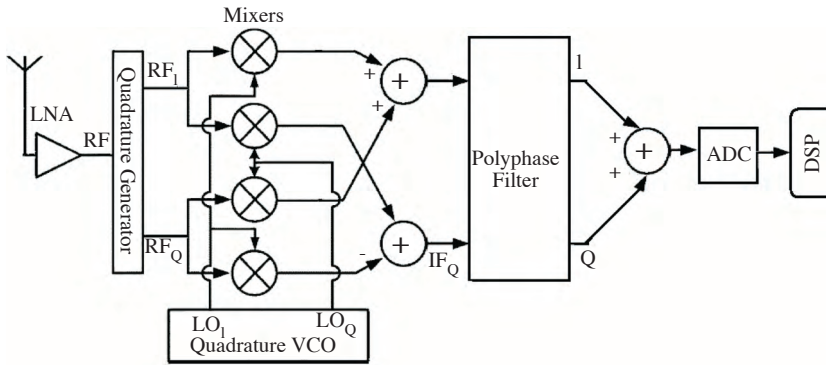


Figure 2. Block diagram of the low-IF receiver architecture.

The polyphase filters have 2 fully differential inputs (I_i and Q_i) and 2 fully differential outputs (I_o and Q_o). Therefore, they are defined by 4 transfer functions. These transfer functions are obtained from the set of independent linear combinations of each input and each output.

To perform image rejection in a low-IF receiver, the filter must have a passband from positive to positive frequencies, an attenuation from negative to negative frequencies, and no signal transfer from positive to negative or negative to positive frequencies. The transfer functions and the circuit synthesis of such a filter can be found by performing a linear frequency transformation on a low-pass filter characteristic.

$$H_{LP}(j\omega) = \frac{1}{1 + j\omega/\omega_o}, H_{BP}(j\omega) = \frac{1}{1 + j(\omega - \omega_c)/\omega_o}, \tag{3}$$

where ω_o is the cutoff frequency of the low-pass filter and ω_c is the center frequency of the band-pass filter.

It should be noted that this transformation makes $H_{BP}(j\omega)$ different for positive and negative frequencies. The realization of this transfer function is given in Figure 3. Higher order filters can be realized as cascade connections of these stages, and then every stage realizes a frequency-translated pole of the low-pass transfer function.

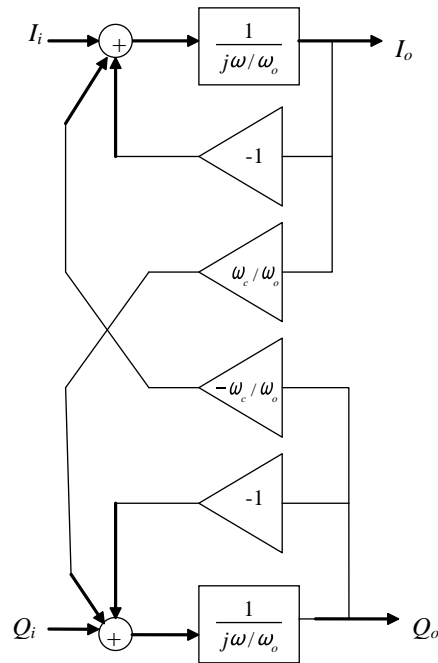


Figure 3. Block diagram of a first-order (single stage) polyphase filter.

From the block diagram in Figure 3, the input and output relations can be found, as follows:

$$\begin{bmatrix} I_i \\ Q_i \end{bmatrix} = \begin{bmatrix} 1 + j\omega/\omega_o & \omega_c/\omega_o \\ -\omega_c/\omega_o & 1 + j\omega/\omega_o \end{bmatrix} \begin{bmatrix} I_o \\ Q_o \end{bmatrix}. \quad (4)$$

Figure 4 gives the active-RC implementation of Figure 3.

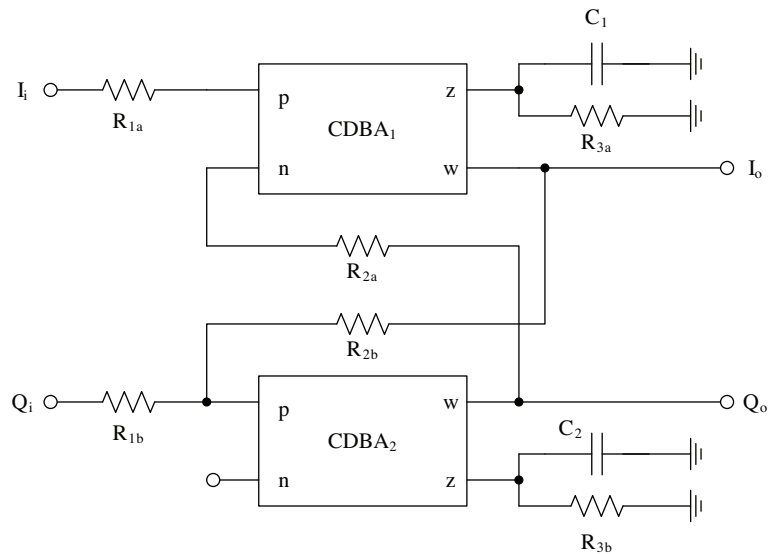


Figure 4. Active-RC implementation of polyphase filter.

Routine analysis of the above circuit yields:

$$\begin{bmatrix} I_i \\ Q_i \end{bmatrix} = \begin{bmatrix} (1 + sR_{3a}C_1)\frac{R_{1a}}{\alpha_{p1}\beta_1R_{3a}} & \frac{\alpha_{n1}R_{1a}}{\alpha_{p1}R_{2a}} \\ -\frac{R_{1b}}{R_{2b}} & (1 + sR_{3b}C_2)\frac{R_{1b}}{\alpha_{p2}\beta_2R_{3b}} \end{bmatrix} \begin{bmatrix} I_o \\ Q_o \end{bmatrix}. \quad (5)$$

Rearranging Eq. (3), the input-to-output voltage transfer functions can be found as:

$$\begin{bmatrix} I_o \\ Q_o \end{bmatrix} = \frac{1}{\Delta} \begin{bmatrix} \frac{R_{1b}(1+sR_{3b}C_2)}{\alpha_{p2}\beta_2R_{3b}} & -\frac{\alpha_{n1}R_{1a}}{\alpha_{p1}R_{2a}} \\ \frac{R_{1b}}{R_{2b}} & \frac{R_{1a}(1+sR_{3a}C_1)}{\alpha_{p1}\beta_1R_{3a}} \end{bmatrix} \begin{bmatrix} I_i \\ Q_i \end{bmatrix}, \quad (6)$$

where $\Delta = \frac{R_{1a}R_{1b}}{\alpha_{p1}\alpha_{p2}} \left\{ \frac{(1+sR_{3a}C_1)(1+sR_{3b}C_2)}{\beta_1\beta_2R_{3a}R_{3b}} + \frac{\alpha_{n1}\alpha_{p2}}{R_{2a}R_{2b}} \right\}$.

Comparison of Eqs. 4 and 5 shows that the passive components should be chosen as $R_{1a} = R_{1b} = R_{3a} = R_{3b} = R$, $R_{2a} = R_{2b} = R/b$, and $C_1 = C_2 = C$ in order to realize the true polyphase filter, where:

$$\omega_o = \frac{1}{RC} \text{ and } \frac{\omega_c}{\omega_o} = b. \quad (7)$$

Therefore, the input-to-output voltage transfer matrix can be reduced to:

$$\begin{bmatrix} I_o \\ Q_o \end{bmatrix} = \frac{1}{\Delta} \begin{bmatrix} \frac{(1+sRC)}{\alpha_{p2}\beta_2} & -\frac{\alpha_{n1}b}{\alpha_{p1}} \\ b & \frac{(1+sRC)}{\alpha_{p1}\beta_1} \end{bmatrix} \begin{bmatrix} I_i \\ Q_i \end{bmatrix}, \quad (8)$$

where $\Delta = \frac{1}{\alpha_{p1}\alpha_{p2}} \left\{ \frac{(1+sRC)^2}{\beta_1\beta_2} + \alpha_{n1}\alpha_{p2}b^2 \right\}$.

The polyphase filter function H_p is equal to $(H_{11} + H_{22})/2 + j(H_{12} - H_{21})/2$ and the mismatch function H_m equals $(H_{11} - H_{22})/2 + j(H_{12} + H_{21})/2$. From Eq. (6), it follows that:

$$H_p = \frac{1}{\Delta} \left[(1 + sRC) \frac{\alpha_{p1}\beta_1 + \alpha_{p2}\beta_2}{2\alpha_{p1}\alpha_{p2}\beta_1\beta_2} - jb \left(\frac{\alpha_{p1} + \alpha_{n1}}{2\alpha_{p1}} \right) \right], \quad (9a)$$

$$H_m = \frac{1}{\Delta} \left[(1 + sRC) \frac{\alpha_{p1}\beta_1 - \alpha_{p2}\beta_2}{2\alpha_{p1}\beta_1\alpha_{p2}\beta_2} + jb \left(\frac{\alpha_{p1} - \alpha_{n1}}{2\alpha_{p2}} \right) \right]. \quad (9b)$$

The ideal conditions $\alpha_{n1} = \alpha_{n2} = \alpha_{p1} = \alpha_{p2} = \beta_1 = \beta_2 = 1$ of the CDBA reduce Eqs. (6), (7), and (8) to:

$$\begin{aligned} \begin{bmatrix} I_o \\ Q_o \end{bmatrix} &= \frac{1}{(1 + sRC)^2 + b^2} \begin{bmatrix} 1 + sRC & -b \\ b & 1 + sRC \end{bmatrix} \begin{bmatrix} I_i \\ Q_i \end{bmatrix} \\ &= \frac{1}{(1 + \frac{s}{\omega_o})^2 + (\frac{\omega_c}{\omega_o})^2} \begin{bmatrix} 1 + \frac{s}{\omega_o} & -\frac{\omega_c}{\omega_o} \\ \frac{\omega_c}{\omega_o} & 1 + \frac{s}{\omega_o} \end{bmatrix} \begin{bmatrix} I_i \\ Q_i \end{bmatrix}, \end{aligned} \quad (10)$$

$$H_p = \frac{1}{(1 + sRC)^2 + b^2} [(1 + sRC) - jb]$$

$$= \frac{1}{(1 + \frac{s}{\omega_o})^2 + (\frac{\omega_c}{\omega_o})^2} [(1 + \frac{s}{\omega_o}) - j \frac{\omega_c}{\omega_o}], \quad (11a)$$

$$H_m = 0, \quad (11b)$$

respectively. Since $H_m = 0$ in the ideal case, the proposed circuit of Figure 4 realizes a true polyphase filter with the transfer function $H_p(s)$ in Eq. (11a).

For the quadrature signal generation, sequence-symmetric polyphase networks can be employed as a generalized structure. Consider the single-stage 4-phase network with a positive sequence transfer function $H_p(\omega)$ and a negative sequence transfer function $H_p(-\omega)$. The network is driven by only 2 phases, representing a differential input signal, if we take the in-phase and quadrature-phase components of the output phases to be V_I and V_Q , respectively. The voltage transfer ratio is then defined as [6]:

$$h(s) = -j \frac{H_p(s) - H_p(-s)}{H_p(s) + H_p(-s)}. \quad (12)$$

Substituting Eqs. (9) and (12), the voltage transfer function is obtained as:

$$h(s) = sRC \frac{\frac{\alpha_{p1}\beta_1 + \alpha_{p2}\beta_2}{2\alpha_{p1}\beta_1\alpha_{p2}\beta_2} \left[b \left(\frac{\alpha_{n1} + \alpha_{p1}}{2\alpha_{p1}} \right) - j \frac{\alpha_{p1}\beta_1 + \alpha_{p2}\beta_2}{2\alpha_{p1}\beta_1\alpha_{p2}\beta_2} \right]}{\left(\frac{\alpha_{p1}\beta_1 + \alpha_{p2}\beta_2}{2\alpha_{p1}\beta_1\alpha_{p2}\beta_2} \right)^2 + b^2 \left(\frac{\alpha_{n1} + \alpha_{p1}}{2\alpha_{p1}} \right)^2}, \quad (13a)$$

which is equal to:

$$h(s) = sRC \frac{b - j}{1 + b^2} \quad (13b)$$

in the ideal case.

3. Simulation results and discussion

The proposed filter configuration, shown in Figure 4, was verified using a CMOS realization of the CDBA with the same CMOS implementation and parameters of the CDBA as in [27]. For these simulations, the passive element values were chosen as $R_{1a} = R_{1b} = R_{3a} = R_{3b} = R = 2 \text{ k}\Omega$, $R_{2a} = R_{2b} = R/b = 1 \text{ k}\Omega$, and $C_1 = C_2 = C = 50 \text{ pF}$. Therefore, $b = R_{1a}/R_{2a} = 2$, $\omega_o = 1/RC = 10 \text{ Mrad/s}$, and $\omega_c = b \omega_o = 5 \text{ Mrad/s}$.

With the above chosen parameters, a comparison of the simulation results with the theoretical results is shown in Figure 5. The discrepancies between the simulation and the theoretical results were as follows. The maximum peak attenuations (peak frequencies) for the simulation and the theoretical results, respectively, were: -4.17 dB (3.4674 MHz) and -5.2 dB (3.4674 MHz) for Figure 5a, -5.19 dB (2.884 MHz) and -6.02 dB (2.7542 MHz) for Figure 5b, -5.207 dB (2.884 MHz) and -6.02 dB (2.7542 MHz) for Figure 5c, and -3.467 dB (4.180 MHz) and -5.2 dB (3.4674 MHz) for Figure 5d. The discrepancies between the simulation and the theoretical results were less than 1 dB up to 60 MHz.

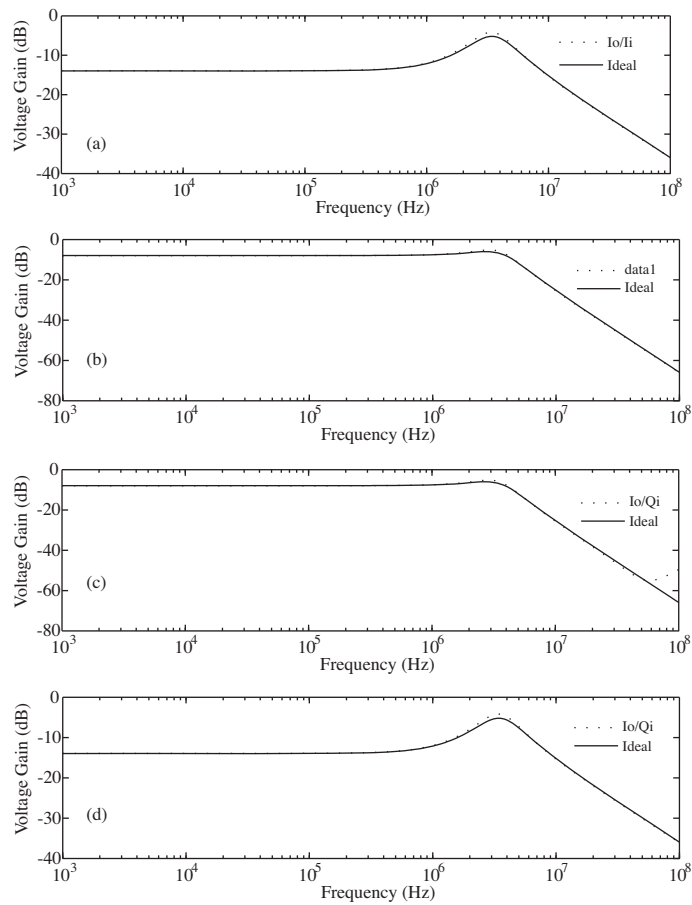


Figure 5. Frequency responses of the proposed polyphase filter.

The transient response for Q_o and I_o outputs of the proposed polyphase filter can be seen in Figure 6. For these simulations, input signals were taken as a sinusoidal voltage signal with a peak value of 100 mV and 3 MHz of frequency. The harmonic analysis of the steady state outputs revealed 0.22% and 0.14% for I_o and Q_o outputs, respectively.

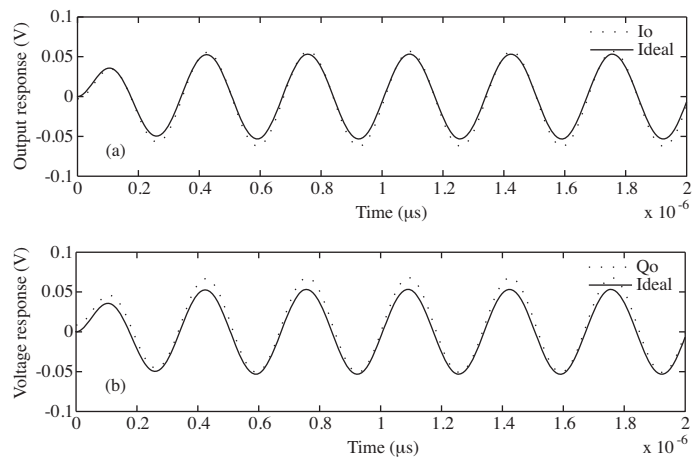


Figure 6. Transient responses of the proposed polyphase filter.

Figure 7 shows the comparison of simulated and theoretical results of the phase responses of the I_o and Q_o outputs. It appears from Figure 7 that the theoretical and simulated results are in good agreement, originating from the nonidealities of the CDBA.

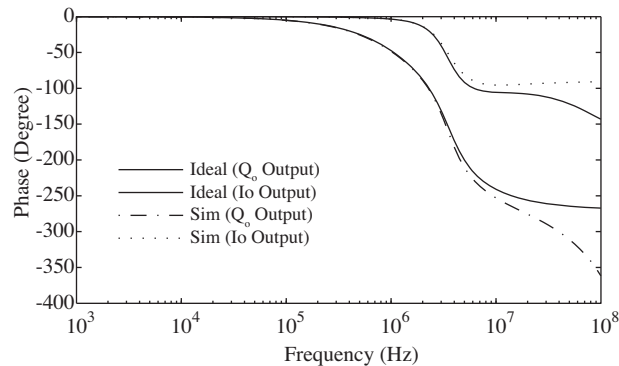


Figure 7. Phase characteristics of the theoretical and simulated polyphase filter in Figure 4.

4. Conclusions

An active polyphase filter section implemented with a CDBA was presented. It used 6 resistors, 2 capacitors, and 2 CDBAs. Although matching of the used resistors was required for the realization, this is a common feature in many circuits and can be handled easily [9-19].

The proposed structure has the following advantages. First, it is suitable for low-IF receivers. Second, increasing the number of cascading sections, any higher order polyphase filter can be realized. Third, it requires only 2 active components. Fourth, all capacitors are grounded, which is more suitable for IC technology. Fifth, all resistors are also grounded or virtually grounded, since the input terminals of the CDBAs are virtually grounded. Sixth, a true polyphase filter is achieved with the proposed structure; since most of the nonideal parameters have symmetrical properties tending to cancellation in the derived equations, mismatching is almost zero.

The above properties, most of which were well verified by the PSpice simulation, make the proposed filter attractive for circuit designers and engineers.

References

- [1] F. Behbahani, Y. Kishigami, J. Leete, A.A. Abidi, "CMOS mixers and polyphase filters for large image rejection", IEEE Journal of Solid-State Circuits, Vol. 36, pp. 873-887, 2001.
- [2] B.J. Minnis, P.A. Moore, "Non-complex signal processing in a low-IF receiver", IEE Proceedings Circuits Devices Systems, Vol. 149, pp. 322-330, 2002.
- [3] J. Crols, M. Steyeart, CMOS Wireless Transceiver Design, Kluwer Academic Publishers, 1997.
- [4] M.A. Gingell, Symmetrical polyphase network, British Patent 1174710, June 1968.
- [5] M.A. Gingell, "Single sideband modulation using sequence asymmetric polyphase networks", Elect. Commun., Vol. 48, pp. 21-25, 1973.
- [6] T. Hornak, "Using polyphase filters as image attenuators", RF Design, pp. 26-34, 2001.

- [7] F. Behbahani, J. Leete, Y. Kishigami, A. Roithmeier, K. Hoshino, A.A. Abidi, "A 2.4 GHz low-IF receiver for wideband WLAN in 0.6 μm CMOS architecture and front-end", IEEE Journal of Solid-State Circuits, Vol. 35, pp. 1908-1916, 2000.
- [8] S.H. Galal, H.F. Ragaie, M.S. Tawfik, "RC sequence asymmetric polyphase networks for RF integrated transceivers", IEEE Transactions on Circuits and Systems-II: Analog and Digital Signal Processing, Vol. 47, pp. 18-27, 2000.
- [9] J. Crols, M. Steyaert, "An analog integrated polyphase filter for high performance low-IF receiver", Symposium on VLSI Circuits Digest of Technical Papers, Kyoto, Japan, pp. 87-88, 1995.
- [10] E. Stikvoort, "Polyphase filter section with OPAMPs", IEEE Transactions on Circuits and Systems-II: Analog and Digital Signal Processing, Vol. 50, pp. 376-378, 2003.
- [11] T. Hornak, "Using polyphase filter as image attenuators", RF Design, pp. 26-34, 2001.
- [12] P. Andreani, S. Mattisson, B. Essink, "A CMOS gm-C polyphase filter with high image band rejection", Proceedings of the European Solid State Circuits Conference, pp. 244-247, 2000.
- [13] C. Muto, "A new extended frequency transformation for complex analog filter design", IEICE Transaction on Fundamentals, Vol. E83-A, pp. 934-940, 2000.
- [14] B. Shi, W. Shan, P. Andreani, "A 57-dB image band rejection CMOS gm-C polyphase filter with automatic frequency tuning for Bluetooth", IEEE International Symposium on Circuits and Systems, Vol. 5, pp. 169-172, 2002.
- [15] T. Melly, E.L. Roux, D. Ruffieux, V. Peiris, "A 0.6mA, 0.9V 100MHz FM front-end in a 0.18 μm CMOS-D technology", Proceedings of the European Solid State Circuits Conference, pp. 417-420, 2003.
- [16] C.Y. Chou, C.Y. Wu, "The design of a new wideband and low-power CMOS active polyphase filter for low-IF receiver applications", Proceedings of the IEEE Asia Pacific Conference on Circuit and Systems, Vol. 1, pp. 241-244, 2002.
- [17] X. Zhang, N. Kambayashi, Y. Shinada, "A realization of active current-mode resonator with complex coefficients using CCII's", IEICE Transactions on Fundamentals, Vol. E80-A, pp. 413-415, 1997.
- [18] M. Ün, "Implementation of polyphase filter section with CFAs", Frequenz, Vol. 58, pp. 221-224, 2004.
- [19] M. Ün, "Analysis of polyphase filter section with CFAs", WSEAS Trans. on CAS, Vol. 2, p. 421, 2003.
- [20] C. Toumazou, F.J. Lidgley, D.G. Haigh, Analogue IC Design: The Current Mode Approach, London, Peter Peregrinus, 1990.
- [21] D.C. Wandsworth, "Accurate current conveyor integrated circuits", Electronics Letters, Vol. 25, pp. 1251-1252, 1989.
- [22] B. Wilson, "Recent developments in current mode circuits", IEE Proc. G, Vol. 137, pp. 63-67, 1990.
- [23] U. Kumar, S.K. Shukla, "Recent developments in current conveyors and their applications", IEE Proc. G., Vol. 16, pp. 47-52, 1985.
- [24] X. Zhang, N. Kambayashi, Y. Shinada, "A realization of active current-mode resonator with complex coefficients using CCII's", IEICE Transactions on Fundamentals, Vol. E80-A, pp. 413-415, 1997.
- [25] C. Acar, S. Ozuguz, "A new versatile building block: current differencing buffered amplifier suitable for analog signal processing filters", Microelectronics J., Vol. 30, pp. 157-160, 1999.

- [26] K. Manetakis, C. Toumazou, "Current-feedback opamp suitable for analog signal-processing filters", *Electronics Letters*, Vol. 32, pp. 1090-1092, 1996.
- [27] C. Acar, H. Sedef, "Realization of nth-order current transfer function using current-differencing buffered amplifiers", *Int. J. of Electronics*, Vol. 90, pp. 277-283, 2003.
- [28] A.Ü. Keskin, C. Aydın, E. Hancıoğlu, C. Acar, "Quadrature oscillators using current differencing buffered amplifiers", *Frequenz*, Vol. 60, pp. 57-59, 2006.
- [29] W. Tangsrirat, D. Prasertsom, T. Piyatat, W. Surakamponorn, "Single-resistance-controlled quadrature oscillator using current differencing buffered amplifiers", *International Journal of Electronics*, Vol. 95, pp. 1119-1126, 2008.
- [30] A.Ü. Keskin, E. Hancıoğlu, "Current-mode multifunction filter using two CDBAs", *AEU-Int. J. Electronics and Communications*, Vol. 59, pp. 495-498, 2005.
- [31] W. Tangsrirat, K. Klahan, K. Kaewdang, W. Surakamponorn, "Low-voltage wide-band NMOS-based current differencing buffered amplifier", *ECTI Transactions on Electrical Eng., Electronics, and Communications*, Vol. 2, pp. 15-22, 2004.
- [32] A.U. Keskin, E. Hancıoglu, "CDBA-based synthetic floating inductance circuits with electronic tuning properties", *ETRI Journal*, Vol. 27, pp. 239-242, 2005.